

## Mechanism for Peroxide Cross-Linking of EPDM Rubber from MAS $^{13}\text{C}$ NMR Spectroscopy

R. A. Orza,<sup>†,‡</sup> P. C. M. M. Magusin,<sup>\*,†</sup> V. M. Litvinov,<sup>‡,§</sup> M. van Duin,<sup>⊥</sup> and M. A. J. Michels<sup>†</sup>

<sup>†</sup>Eindhoven University of Technology, P.O. Box 513, 5600 MB Eindhoven, The Netherlands, <sup>‡</sup>Dutch Polymer Institute, P.O. Box 902, 5600 AX Eindhoven, The Netherlands, <sup>§</sup>DSM Research, P.O. Box 18, 6160 MD Geleen, The Netherlands, and <sup>⊥</sup>DSM Elastomers Global R&D, P.O. Box 1130, 6160 BC Geleen, The Netherlands

Received July 25, 2009; Revised Manuscript Received October 8, 2009

**ABSTRACT:** Detailed information about the chemical role of the third monomer 5-ethylidene-2-norbornene (ENB) in EPDM during peroxide cross-linking has been obtained by use of MAS  $^{13}\text{C}$  NMR spectroscopy and  $^1\text{H}$  NMR  $T_2$  relaxometry. Advanced  $^{13}\text{C}$  NMR techniques like INADEQUATE and TOCSY applied to a special EPDM grade with  $^{13}\text{C}$ -labeled ENB reveal a large number of new aliphatic and olefinic signals as well as indications for oxidation. The ENB unit is involved in cross-linking reactions not only (i) via addition of macroradicals to the pendent ENB unsaturation yielding aliphatic cross-link structures but also (ii) via combination of ENB-derived allyl radicals resulting in cross-link structures with intact unsaturation. The latter represents a novel pathway in the mechanism for peroxide curing of EPDM.

### Introduction

Ethylene–propylene–diene terpolymers (EPDM) represent a class of elastomers with a saturated backbone, which makes these materials resistant against oxygen, ozone, heat, and UV light and therefore particularly suited for outdoor applications, such as automotive sealing systems and roofing for buildings.<sup>1,2</sup> Chemical cross-linking of EPDM is necessary to form a mechanically stable rubber network with optimal tensile and elastic properties. In general, EPDM is either cross-linked by sulfur vulcanization or peroxide curing.<sup>3</sup> For that purpose, a small amount of a nonconjugated diene monomer, such as 5-ethylidene-2-norbornene (ENB), dicyclopentadiene, or 5-vinyl-2-norbornene, is commonly copolymerized to provide unsaturation randomly attached along the polymer chain. Incorporation of the diene monomer into EPDM enables sulfur vulcanization and enhances the peroxide curing efficiency.

Sulfur vulcanization results in sulfur cross-links between the polymer chains, providing interchain bonds which are flexible but have limited thermal stability.<sup>3</sup> As the number of sulfur atoms in a sulfur cross-link increases, the thermal stability decreases. Sulfur vulcanization is a robust technology and is practiced in a wide variety of vulcanization processes, such as compression and injection molding, extrusion, and hot-air autoclaves. A major advantage of this type of cross-linking is that by varying the sulfur curatives formulation, the cross-linking kinetics and the final cross-link density can be tuned to a broad range of cross-linking technologies and applications. The chemical mechanism of sulfur vulcanization of EPDM has been investigated in detail for low-molecular-weight model compounds<sup>4</sup> and by use of  $^{13}\text{C}$  NMR applied to a special EPDM grade with  $^{13}\text{C}$ -labeled ENB.<sup>5</sup> As shown in both model and polymer studies, sulfur vulcanization involves substitution at the allyl positions next to the residual unsaturation in ENB–EPDM, while the double bond itself is not converted.

As opposed to sulfur vulcanization, the cross-links provided by peroxide cure consist of carbon–carbon bonds, which have the same bond strength as the C–C bonds in the polymer backbone. Therefore, peroxide cure provides better heat aging properties and high-temperature compression set. However, peroxide cure tends to be less easy to control. The resulting rubber networks are believed to be more heterogeneous. Contact with air results in products with sticky surfaces, which is probably caused by oxygen inhibition of the free-radical cross-linking at the surface, degradation of polymer chains, and/or formation of polar oxidation products. Thus, unlike sulfur vulcanization peroxide cure cannot be performed in hot-air autoclaves.

Peroxide cross-linking covers about 15% of the commercial EP(D)M applications because of the enhanced performance at high temperature. According to the generally accepted mechanism,<sup>3</sup> peroxide curing is initiated by the thermal decomposition of the peroxide. The resulting free radicals subsequently abstract hydrogen atoms from the EPDM polymer, yielding EPDM macroradicals. Since the reactivity of the primary peroxide radicals is high, this step is kinetically determined. Calculations have shown that the hydrogen atoms are mainly abstracted from the aliphatic tertiary and secondary carbon atoms in the EPDM main chain.<sup>6</sup> Once formed, the EPDM macroradicals can give rise to cross-links in two ways. First, they can combine, yielding direct C–C cross-links between the two polymer chains. Second, they can add to a residual EPDM unsaturation. The resulting radical undergoes hydrogen transfer, yielding a cross-link with a diene monomer unit between the two polymer chains and a new EPDM macroradical that can react again. A recent model study with low-molecular-weight compounds has indicated a third pathway, which involves formation of macroradicals at the  $\alpha$  positions next to the unsaturation in the diene units.<sup>7</sup> Indeed, hydrogen atoms at allyl positions next to double bonds are relatively labile because radicals at such positions are stabilized by resonance, as have been observed with ESR.<sup>8</sup>

In our previous work on peroxide-cured EPDM rubber, the cross-link density and network heterogeneity have been studied

\*Corresponding author. E-mail: p.c.m.m.magusin@tue.nl.

by means of  $^1\text{H}$  NMR relaxometry.<sup>9,10</sup> For EPDM/peroxide compositions representative for industrial applications the peroxide efficiency was shown to be  $\sim 50\%$ , the diene conversion was up to  $40\%$ , and the contribution of addition cross-links to the total cross-link density was up to  $40\%$ , the latter two depending on the peroxide content and the diene monomer type and content.

Following on the earlier  $^{13}\text{C}$  NMR study of sulfur-vulcanized EPDM,<sup>5</sup> the aim of this work is to study the chemical structures formed upon peroxide cure of EPDM with ENB as third monomer in more detail. In particular, we want to test the generally accepted mechanism for peroxide cure, in which the pendent unsaturation in EPDM only serves as a site for addition by peroxide-initiated macroradicals. Furthermore, we want to check the relevance of the allyl-combination pathway found in the previous model study<sup>7</sup> for the real EPDM rubber system. Enhanced insight into the chemical reactions occurring during peroxide cross-linking of EPDM is important for a sound understanding of peroxide cross-linking kinetics and structure-properties relationships for the vulcanizates. Magic-angle spinning  $^{13}\text{C}$  NMR spectroscopy and static  $^1\text{H}$  NMR relaxometry were respectively employed to identify the chemical structures formed in peroxide-cured EPDM and to determine the network densities. By monitoring the peak area of the olefinic  $^{13}\text{C}$  resonances of the ENB third monomer at subsequent stages during a stepwise peroxide cure, and by determining the cross-link density at these steps from  $^1\text{H}$  NMR  $T_2$  relaxation, both the ENB conversion and the cross-link density were studied as a function of the curing time, and the correlation between the two was established.  $^{13}\text{C}$  NMR in combination with selective  $^{13}\text{C}$  labeling at strategic carbon positions is powerful for unraveling chemical structures in polymers.<sup>5,11–13</sup> In our current investigation we have studied EPDM with ENB  $^{13}\text{C}$ -enriched at the C2/C8 double bond positions, which leads to strongly enhanced NMR signals and facilitates a successful characterization of the new structures involving the diene unsaturation. In addition, the double labeling at the neighboring C2 and C8 positions permitted the use of  $^{13}\text{C}$ – $^{13}\text{C}$  correlation NMR techniques, such as INADEQUATE and TOCSY.

## Experimental Section

**Materials.**  $^{13}\text{C}$ -Labeled ENB–EPDM. The  $[2,8\text{-}^{13}\text{C}_2]$  ENB–EPDM rubber used in this study has been synthesized by Heinen et al.<sup>11</sup> It has an ethylene to propylene ratio of  $\sim 1.8$ , an ENB content of  $\sim 8\text{ wt } \%$  ( $\approx 670\text{ mmol/kg}$ ), and  $M_w$  of  $4.8 \times 10^5\text{ g/mol}$ . ENB is incorporated in the polymer through its endocyclic C5/C6 double bond. Because of the limited quantity of labeled EPDM available, EPDM/peroxide compounds were prepared on a small scale via a solution route, and one sample was used for stepwise vulcanization. NMR experiments were performed after each vulcanization step. 100 mg of EPDM compound with 4.3 wt % di(*tert*-butylperoxyisopropyl)benzene from Across was prepared by dissolution in hexane followed by evaporation and drying at  $90\text{ }^\circ\text{C}$  under vacuum. Cross-linking was performed in a hot press at  $175\text{ }^\circ\text{C}$  either in a single step of 17 min or in a stepwise manner for accumulative times of 3, 6, 9, and 19 min. The peroxide half-life time at  $175\text{ }^\circ\text{C}$  is 1 min.<sup>14</sup> After every cross-link step the EPDM sample was taken out of the hot press as a 1 mm thick circular film with a diameter of 2 cm and left to cool within a few minutes to room temperature in air. For probing the effect of air-induced oxidation in the absence of peroxide, a 1 mm thick EPDM sheet with a diameter of 2 cm was exposed to air in an oven at  $175\text{ }^\circ\text{C}$  for 2 h.

**NMR Characterization.**  $^{13}\text{C}$  NMR Hahn Echo. Magic-angle spinning (MAS)  $^{13}\text{C}$  NMR spectra were recorded on a Bruker DMX500 spectrometer equipped with a 4 mm MAS probehead and operating at a  $^{13}\text{C}$  NMR frequency of 125 MHz. The sample rotation rate was 4 or 8 kHz. To suppress baseline artifacts

resulting from pulse leakage into the NMR signal, direct-excitation  $^{13}\text{C}$  NMR spectra with proton decoupling were recorded by use of the Hahn-echo pulse sequence  $90^\circ\text{--}\tau\text{--}180^\circ\text{--}\tau$  with a  $90^\circ$  pulse of  $5\text{ }\mu\text{s}$  and echo time  $2\tau = 6\text{ }\mu\text{s}$ . Such echo time is short compared to the sample rotation time (125 or 250  $\mu\text{s}$ ) and therefore does not cause significant dephasing of the spinning sidebands. The relaxation delay between subsequent scans was 5 s, which in comparison with test experiments at 10 s proved long enough to avoid saturation and transient NOE effects. The experiments were performed at room temperature and at  $90\text{ }^\circ\text{C}$ . The  $^{13}\text{C}$  NMR signal of adamantane at 38.56 ppm was used as a reference.

**1D and 2D INADEQUATE.** The 1D and 2D INADEQUATE spectra were recorded at  $90\text{ }^\circ\text{C}$  on a Bruker DMX500 spectrometer using a 4 mm MAS probehead and the pulse sequence  $90^\circ\text{--}\tau\text{--}180^\circ\text{--}\tau\text{--}90^\circ\text{--}t_1\text{--}90^\circ\text{--}\tau\text{--}180^\circ\text{--}\tau\text{--}90^\circ\text{--}\text{acquisition}$ . The theoretically optimal value for the delay  $\tau$  in this type of experiments is  $1/(4J)$  with  $J$  the  $^{13}\text{C}$ – $^{13}\text{C}$  scalar coupling constant. The  $\tau$  value in our experiments was  $\sim 4\text{ ms}$ , which represents a compromise between the typical  $J$  constant for  $\text{sp}_2\text{--}\text{sp}_2$  coupling ( $\sim 75\text{ Hz}$ ) and  $\text{sp}_3\text{--}\text{sp}_3$  coupling ( $\sim 40\text{ Hz}$ ). No strong  $\tau$  dependence has been observed in test experiments. For 1D INADEQUATE a constant  $t_1$  delay was chosen as small as possible for sufficient pulse separation, 3  $\mu\text{s}$ , and a relaxation delay of 2.5 s. To be able to detect the  $^{13}\text{C}$  NMR signals down to a few percent, typically 25 000 scans were recorded. The typical time to record a 1D INADEQUATE spectrum was 18 h. For 2D INADEQUATE  $t_1$  was systematically incremented by 10  $\mu\text{s}$  up to 5 ms, and the relaxation delay was 2 s. Special pulse phase lists were employed to reduce the artifacts arising from the incomplete magnetization recovery during the relatively short inter-scan delay.<sup>15</sup> Time-proportional phase incrementing (TPPI) was used for phase-sensitive detection in the indirect domain.

**2D TOCSY.** Total correlation spectroscopy (TOCSY) was carried out at  $90\text{ }^\circ\text{C}$  by use of the pulse sequence  $90^\circ\text{--}t_1\text{--}90^\circ\text{--}p_{\text{mix}}\text{--}90^\circ\text{--}t_2$  with  $p_{\text{mix}}$  the standard DIPSI-2 multipulse scheme for homonuclear Hartmann–Hahn mixing.<sup>16</sup> The overall duration of  $p_{\text{mix}}$  was 30 ms. TPPI was used again for phase-sensitive detection in the indirect domain.

**$^1\text{H}$  NMR Hahn-Echo Relaxometry.** The  $^1\text{H}$  transverse magnetization relaxation of the stepwise-cross-linked EPDM was measured on a Bruker Minispec MQ-20 spectrometer operating at a  $^1\text{H}$  frequency of 20 MHz. This spectrometer was equipped with a BVT-3000 variable temperature unit. All experiments were performed at  $90\text{ }^\circ\text{C}$ .

The decay of the transverse magnetization was measured with the Hahn-echo pulse sequence:  $90^\circ_x\text{--}t_{\text{HE}}\text{--}180^\circ_y\text{--}t_{\text{HE}}\text{--}[\text{acquisition of the amplitude of an echo maximum } A(t)]$ , where  $t_{\text{HE}} \geq 35\text{ }\mu\text{s}$ . This pulse sequence eliminates the magnetic field and chemical shift inhomogeneities and allows robust and quantitative measurements. An echo signal is formed with a maximum at time  $t = 2t_{\text{HE}} + (t_{90} + t_{180})/2$  from the beginning of the first pulse, where  $t_{90}$  and  $t_{180}$  are the durations of the  $90^\circ$  and  $180^\circ$  pulses, respectively ( $t_{90} = 2.8\text{ }\mu\text{s}$ ). By variation of the pulse spacing  $t_{\text{HE}}$  in the sequence, the amplitude of the transverse magnetization is measured as a function of the echo time  $2t_{\text{HE}}$ .

The high-temperature limit value  $T_2^{\text{pl}}$  of the transversal relaxation time  $T_2$  is a measure for the cross-link density.<sup>17–19</sup> The  $T_2^{\text{pl}}$  value is related to the number of statistical segments between chemical and physical network junctions.<sup>18,20</sup> Equations 1 and 2 in ref 9 were used to estimate the total network density  $D_{\text{tot}}$  from the  $T_2$  plateau value  $T_2^{\text{pl}}$ .

## Results

**Overall  $^{13}\text{C}$  NMR Analysis.** The main goal of this study is to get insight into the structures of the chemical cross-links and other chemical structures formed during peroxide cure of EPDM. The unsaturation of ENB is essential in peroxide cross-linking, but because of the low content

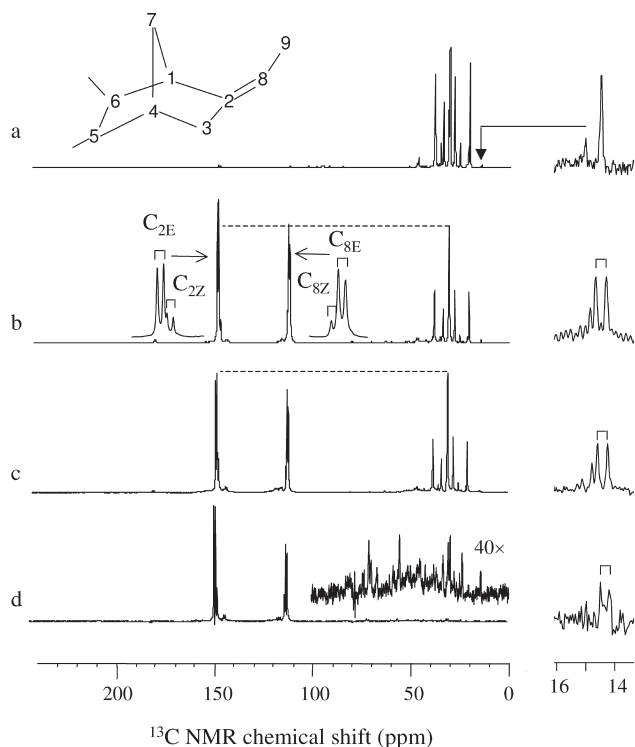


**Figure 1.** MAS <sup>13</sup>C NMR spectra of EPDM. (left) Hahn-echo spectra of (a) cross-linked nonlabeled EPDM, (b) non-cross-linked EPDM with <sup>13</sup>C labels at the C2 and C8 positions in ENB, and (c) cross-linked labeled EPDM as well as (d) the INADEQUATE spectrum of the latter. The insets in (a) show the carbon positions in the third monomer 5-ethylidene-2-norbornene (ENB), in (b) the four doublets arising from the scalar <sup>13</sup>C–<sup>13</sup>C coupling between the <sup>13</sup>C nuclei at positions C2 and C8 in the E and Z form of ENB, and in (d) the magnified (mainly) aliphatic signals of the <sup>13</sup>C–<sup>13</sup>C pairs after cross-linking. The horizontal broken lines in (b) and (d) are a guide for the eye to illustrate the relative decrease of the double-bond signal upon cross-linking. (right) Expanded 12–17 ppm regions with the natural-abundance signals from the methyl moieties at the chain ends and the C9 position in ENB. The C9 methyl doublets for labeled EPDM arise from coupling to the neighboring <sup>13</sup>C nucleus at C8 in ENB.

(usually < 10 wt %, corresponding to < 1.2 C=C bond per 100 C atoms), it is difficult to characterize the reaction products at natural-abundance <sup>13</sup>C levels.<sup>21</sup> This is why <sup>13</sup>C labeling is important, since it allows a direct study of the carbon atoms involved in peroxide curing of EPDM. The availability of EPDM with <sup>13</sup>C labels at the C2/C8 double-bond positions in ENB offers a unique opportunity to directly detect reaction products formed during peroxide cross-linking with <sup>13</sup>C NMR spectroscopy. The assignment of the new signals in the spectra was facilitated by the availability of the NMR spectra of the corresponding non-labeled and labeled compounds.<sup>11,22–25</sup> In earlier studies not much attention has been given to these new resonances.<sup>25</sup> We will address this subject in the present article.

<sup>13</sup>C NMR spectra of cross-linked nonlabeled EPDM and <sup>13</sup>C-labeled EPDM before and after cross-linking are shown in Figure 1. Unlike for, e.g., natural rubber,<sup>26</sup> the <sup>13</sup>C NMR spectrum of nonlabeled EPDM is strongly dominated by aliphatic signals from the EPM backbone between 0 and 55 ppm (Figure 1a). On the basis of previous analyses,<sup>27,28</sup> the main signals are assigned to primary (20.6 ppm) and tertiary carbons (33.5 ppm) as well as secondary carbons at various distances from the nearest tertiary carbon along the polymer chain (38.2, 28.0, 30.9, and 30.6 ppm). Although the natural-abundance EPDM serves a convenient reference, the here-reported NMR study focuses on ENB–EPDM with

<sup>13</sup>C labels at the C2 and C8 positions in ENB. Therefore, wherever in the remainder of this paper we refer to EPDM samples investigated with NMR, the reader may assume that it was <sup>13</sup>C labeled, unless specified differently. The C2/C8 labeling gives rise to strongly enhanced olefinic signals at 147 and 111 ppm, respectively (Figure 1b). The overall olefinic peak area (100–160 ppm) in the spectrum of non-cross-linked labeled EPDM relative to the peak area between 19 and 23 ppm from the methyl signals of the propylene units in EPDM equals  $16.3 \pm 0.5$ , which agrees well with the composition of the EPDM grade in this study (17.0). Closer inspection reveals two pairs of overlapping doublets (inset in Figure 1b). The larger doublets at 147.1 and 111.3 ppm with a <sup>13</sup>C–<sup>13</sup>C coupling of 76 Hz are assigned to the E isomer of ENB in the EPDM and the smaller doublets at 146.2 and 111.9 ppm with a coupling constant of 78 Hz to the Z isomer.<sup>11</sup> Lineshape deconvolution indicates an E/Z ratio of ~5.7, which is somewhat higher than originally reported for this particular <sup>13</sup>C-labeled EPDM grade. Analysis of the spectrum of cross-linked labeled EPDM (Figure 1c) shows a decrease of the total olefinic peak area to  $11.4 \pm 0.4$  relative to the methyl peak area between 19 and 23 ppm. As follows from peak deconvolution, this decrease is actually the result of a 39% and 28% reduction of the signals from E- and Z-ENB, respectively, combined with the appearance of several small olefinic signals at the foot of the original signals. A more detailed analysis of these new signals will follow later in this paper. At first sight, when comparing the patterns of the major aliphatic signals of EPDM before and after cross-linking, this range of the spectrum seems hardly changed. At closer inspection, however, a kind of “broadening” at the foot of the resonances is evident, which actually contributes significantly to the spectral integral in this range. In fact, parallel to the overall decrease of the olefinic signals, there is an overall increase of the aliphatic peak area (0–55 ppm including the methyl peak area taken as 1) from  $9.6 \pm 0.3$  for non-cross-linked to  $10.6 \pm 0.3$  for cross-linked EPDM. This is consistent with the accepted view that the double bond in ENB becomes saturated during peroxide cross-linking. It is not trivial to resolve these small new signals from under the large natural-abundance <sup>13</sup>C NMR signals of the aliphatic carbon atoms in the rest of the polymer chain. As shown in Figure 1d, the natural-abundance signals are suppressed in a so-called INADEQUATE spectrum. Such a spectrum is recorded with a double-quantum filter which selects the signals of *J*-coupled <sup>13</sup>C–<sup>13</sup>C spin pairs only. The suppression is based on the fact that the statistical occurrence of natural-abundance <sup>13</sup>C–<sup>13</sup>C pairs at neighboring positions along the chain is extremely low. Even with the background suppressed, no signals from the labeled C2 and C8 carbons in new saturated structures are observed with peak heights > 5% of the maximum peak height of the C2 signal at 147 ppm. At higher magnification, however, the <sup>13</sup>C NMR spectra are more informative about the chemistry taking place. This is, for instance, illustrated by the natural-abundance signals at 15.0 and 14.4 ppm from methyl end groups in the polymer chain and C9 methyl moieties in ENB, respectively (Figure 1, right-hand side). The doublet splitting of the 14.4 ppm signal observed for labeled EPDM is characteristic for the sp<sup>2</sup>–sp<sup>3</sup> coupling between the <sup>13</sup>C nuclei at the labeled C8 position and natural-abundant <sup>13</sup>C nuclei at C9. The fact that the signal at 15.0 ppm is absent in the INADEQUATE spectrum confirms its assignment to the chain-end methyl groups. Interestingly, whereas the chain-end methyl signal appears unaffected upon cross-linking, the C9 signal from cross-linked EPDM is lower



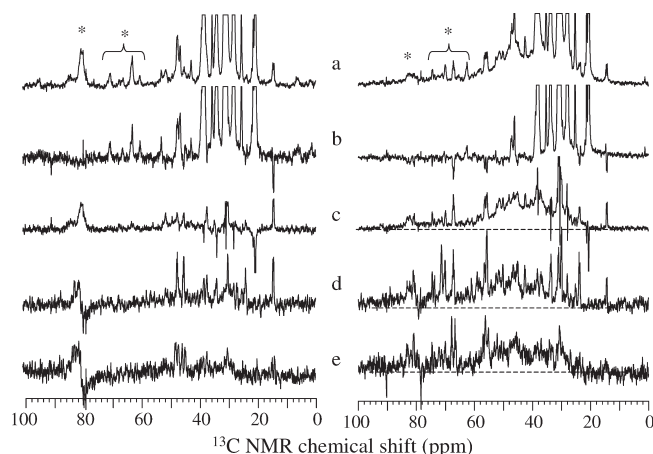


**Figure 2.** Aliphatic and alcohol/ether  $^{13}\text{C}$  NMR signals in Hahn-echo and INADEQUATE spectra of (left) non-cross-linked and (right) peroxide-cross-linked  $^{13}\text{C}$ -labeled EPDM. (a, b) Hahn-echo spectra at echo times 0.5 and 8.5 ms, the latter with negative signals caused by  $^{13}\text{C}$ – $^{13}\text{C}$  coupling. (c) Difference spectrum emphasizing the signals from  $^{13}\text{C}$  nuclei at or next to the  $^{13}\text{C}$ -labeled positions as well as those with short coherence times  $T_2$  as a result of the polymer-chain immobilization caused by cross-linking. (d, e) INADEQUATE spectra with and without proton decoupling, the first to identify signals at or next to the labeled positions and the latter to determine the carbon type. All spectra in this figure were recorded at 90 °C and a sample-rotation rate of 4 kHz. The positions of spinning sidebands are marked with a star (\*) in the upper traces.

than that of EPDM prior to peroxide curing. This will be explained later.

There are two possible explanations for the “broadening” observed in the  $^{13}\text{C}$  NMR spectrum of cross-linked EPDM and the lack of clear aliphatic signals in the INADEQUATE spectrum. On the one hand, it could reflect an immobilized-chain fraction in the heterogeneous network resulting from peroxide cross-linking. Immobilization leads to shorter  $^{13}\text{C}$  spin coherence times  $T_{2\text{C}}$  and thus larger homogeneous line widths. On the other hand, the broadening may also be heterogeneous and the lack of clear INADEQUATE signals could be a result of the isotope scrambling over a large variety of cross-link structures. These two options have been tested by comparing Hahn-echo spectra with short and long echo times  $2\tau$  equal to 0.5 and 8 ms, respectively (Figure 2a, b). Variation of the echo time hardly affects the spectrum of non-cross-linked labeled EPDM (Figure 2a). In contrast, broad components in the 0.5 ms echo spectrum of cross-linked labeled EPDM are absent for  $2\tau = 8$  ms (Figure 2b). This suggests that these are homogeneously broadened signals from  $^{13}\text{C}$  nuclei with short  $T_{2\text{C}}$  times. However, the *inversion* of some signals, such as the narrow C9 signal at 14.4 ppm, cannot be explained by  $T_2$  relaxation. It is caused by  $^{13}\text{C}$ – $^{13}\text{C}$  coupling, which is not refocused in the Hahn echo. The Hahn-echo difference spectra (Figure 2c) thus contain a mixture of signals from  $^{13}\text{C}$  nuclei with short  $T_{2\text{C}}$  times or  $^{13}\text{C}$ – $^{13}\text{C}$  coupling. These spectra may be compared with INADEQUATE spectra, which are primarily selective for carbon nuclei with  $^{13}\text{C}$ – $^{13}\text{C}$  coupling but also require long  $T_{2\text{C}}$  values because of the long echo times in the pulse sequence. There is a strong similarity between the Hahn-echo difference spectra and the corresponding INADEQUATE spectra, both with regard to individual positions of the resolved peaks and the continuous range of aliphatic signals that give rise to the broad “hump” between 20 and 50 ppm. Before discussing the spectral changes in more detail, we will discuss the decrease of the ENB unsaturation during peroxide curing, as monitored with  $^{13}\text{C}$  NMR spectroscopy, and

correlate that to the cross-link density, as calculated from  $^1\text{H}$  NMR relaxometry.

**Cross-Link Density and ENB Conversion.** To monitor the network formation and ENB conversion during peroxide cross-linking at 175 °C, an EPDM/peroxide mixture was cured in a stepwise manner times during accumulative times of 3, 6, 9, and 19 min. At the end of every step the mixture was taken from the press and quenched to room temperature. Then, a sample was taken for further study, and the mixture put back into the hot press for the next cure step. These samples representing subsequent cross-link stages were then studied with a combination of static  $^1\text{H}$  NMR  $T_2$  relaxometry and MAS  $^{13}\text{C}$  NMR spectroscopy.

Although the validity of the underlying polymer model and NMR theory has been questioned,<sup>29</sup>  $^1\text{H}$  NMR  $T_2$  relaxometry has proven a valuable tool in practice for obtaining insight into the network density and heterogeneity of cross-linked rubbers.<sup>9,19,30,31</sup> The decay of the  $^1\text{H}$  NMR Hahn echo as a function of the echo time is mainly determined by the anisotropy of the chain mobility and, thus, strongly affected by the cross-link density. The total network density, including the contributions of (chemical) cross-links and (physical) chain entanglements, can be calculated from the plateau value  $T_{2\text{H}}^{\text{pl}}$  at temperatures far above the glass-transition temperature.<sup>9</sup>

From the relaxation experiments the total network density can be calculated, and the chemical cross-link density can be determined by subtracting the entanglement density. Such model of the total network density as the sum of independent chain entanglements and chemical cross-links is based on the assumption that the topology of the polymer chains is not affected by the chemical cross-links (although the nature of the entanglements may change from transient to trapped). As entanglement density, we use a value of 230 mmol/kg determined in our previous study by extrapolating the network density to zero peroxide.<sup>9</sup> This is a more accurate procedure than trying to measure the  $T_{2\text{H}}^{\text{pl}}$  value of EPDM prior to the peroxide cross-linking, since non-cross-linked EPDM has no clear  $T_{2\text{H}}$  plateau.<sup>19</sup> The evolution of the chemical cross-link density, derived from  $T_2$  relaxometry, as a function of cross-linking time is shown in Figure 3. The cross-link density follows a concave curve and is completed after  $\sim 10$  min, which is consistent with the half-life time of 1 min of the peroxide at 175 °C.<sup>14</sup> The final cross-link density of this stepwise cured EPDM,  $\sim 400$  mmol/kg, is higher than the value  $\sim 250$  mmol/kg found in our previous study for single-step cured EPDM with a similar overall ENB content and initial peroxide level.<sup>9</sup> Either the stepwise curing procedure enhances the efficiency of the peroxide (initially present at 130 mmol/kg) or this procedure induces a larger entanglement density than the typical value of 230 mmol/kg found in our previous study of EPDM cured in a single step.

Under proper experimental conditions,  $^{13}\text{C}$  NMR spectroscopy can be employed for quantitative analysis of polymeric compounds.<sup>32–34</sup> Especially in the solid state the  $^{13}\text{C}$  spin–lattice relaxation times  $T_{1\text{C}}$  can be long, and long interscan delays ( $> 5T_{1\text{C}}$ ) should be used to avoid spectral saturation effects. Fortunately, the chain mobility in rubbers far above the glass-transition temperature is high, and the relaxation time  $T_{1\text{C}}$  is therefore relatively short ( $\sim 1$  s). Proton-decoupled  $^{13}\text{C}$  NMR spectra of mobile hydrocarbon systems may be affected by dynamic  $^{13}\text{C}$ – $\{^1\text{H}\}$  NOE effects, which could spoil a quantitative analysis of the signal intensities.<sup>34,35</sup> However, such NOE effects are bounded by the rate at which the  $^{13}\text{C}$  spins relax to thermal equilibrium and therefore are negligible in spectra recorded with interscan delays  $> 5T_{1\text{C}}$ . To study the conversion of the C2/C8

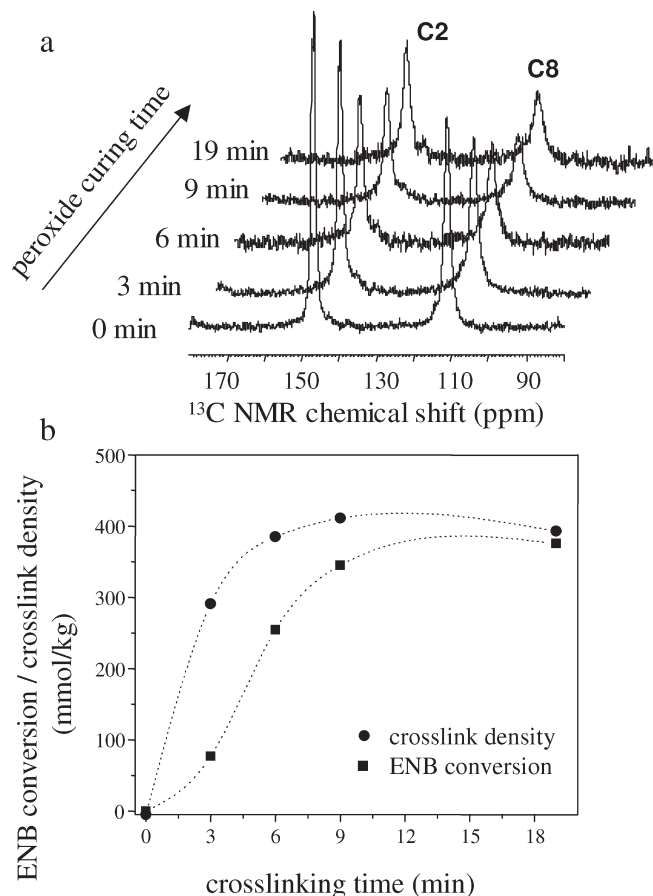


**Figure 3.** (a) Olefinic region in the MAS  $^{13}\text{C}$  NMR spectra of the stepwise cross-linked EPDM at consequent steps in the peroxide cure. (b) Comparison of ENB double-bond conversion from MAS  $^{13}\text{C}$  NMR spectroscopy and cross-link formation from  $^1\text{H}$  NMR relaxometry during the stepwise peroxide cross-linking.

ENB double bond during peroxide cross-linking and to correlate it to the cross-link density, the EPDM/peroxide samples taken from the press at intermediate cross-linking times were also studied with MAS  $^{13}\text{C}$  NMR. The spectra were recorded at 25 °C, instead of the usually elevated temperature, to avoid further cross-linking during the NMR experiment. Tradeoff for the lower measuring temperature is a larger MAS  $^{13}\text{C}$  NMR line width. This is illustrated by the different resolution in the spectra shown in Figures 1 and 3 (top). As a result, it is not possible to distinguish between the olefinic signals from the E- and Z-ENB isomers, nor to recognize the formation of new olefinic signals. Thus, the MAS  $^{13}\text{C}$  NMR spectra at 25 °C yield only rough information about the overall decay of the C2 and C8 signals around 147 and 111 ppm, respectively (Figure 3, top). From the relative decrease of the peak intensities and the starting ENB content, the conversion of the ENB unsaturation can be calculated in similar units as the cross-link density derived from  $^1\text{H}$  NMR  $T_2$  relaxometry (mmol/kg). The data for ENB conversion plotted in Figure 3 are averages for the C2 and C8 peaks. An S-shaped conversion profile is observed, reaching a plateau concentration of  $\sim 380$  mmol/kg converted ENB units at  $\sim 15$  min. This may be compared with the overall ENB concentration  $\sim 670$  mmol/kg in the investigated EPDM grade and indicates a higher ENB conversion in the stepwise cured EPDM sample than in the single-step cured EPDM sample (previous section). Although the relative errors in the cross-link density calculated from  $^1\text{H}$  NMR  $T_2$  relaxation (5% experimental

and 10% model-related errors) and in the ENB conversion estimated from the olefinic  $^{13}\text{C}$  NMR signals (levels off at 15% upon increasing curing time) are significant, it may still be concluded that the cross-link density and the ENB conversion behave differently as a function of time. The cross-link density is higher than the ENB conversion over the whole time interval, although they approach each other upon full curing. Initially, the cross-link density is increasing faster than the conversion of the ENB unsaturation. However, during the later stages of curing the ENB conversion is still continuing, while cross-link formation has leveled off. The fast network formation relative to the double-bond conversion indicates that the initial cross-linking is dominated by combination of the macroradicals produced after the peroxide decomposition, while at a later stage the addition of macroradicals to the ENB unsaturation takes over. Thus, the balance between the combination and addition pathways in the peroxide-cure mechanism changes with time. This makes sense because cross-linking via combination is second order in macroradical concentration and thus predominant when relatively large amounts of peroxide are decomposing. In contrast, cross-linking via addition is first order in macroradical concentration and thus tends to predominate at lower levels of decomposing peroxides, i.e., at later stages in peroxide curing.

At first sight, it may seem from the comparable concentrations of cross-links and converted ENB units after 15 min (Figure 3) that in the final stage almost all cross-links have been formed via addition. However, from the  $T_2$  analysis for fully cured EPM (without ENB) in our previous work,<sup>9</sup> it follows that at 4.3% peroxide the density of cross-links produced via combination equals 130 mmol/kg. Thus, according to the additive model that assumes the density of cross-links formed via combination of EPDM macroradicals, and the density of cross-links formed by addition of EPDM radicals to the ENB unsaturation to be independent of each other, and proved to be successful before,<sup>9</sup> the specific cross-link density arising from the addition route in the fully cured EPDM sample, studied in the present article, equals  $400 - 130 = 270$  mmol/kg. This is significantly lower than the final ENB conversion, 380 mmol/kg. A possible explanation is that the ENB unsaturation is not only converted to saturated cross-links via the addition pathway but that also other reactions occur, which contribute to the conversion of the ENB unsaturation as well. As will follow from detailed analysis of the spectra in the next section, this is indeed the case.

**Detailed Analysis of the  $^{13}\text{C}$  NMR Spectra.** The  $^{13}\text{C}$  NMR spectrum of  $^{13}\text{C}$ -labeled EPDM after cross-linking contains a large variety of new olefinic and aliphatic signals. It is impossible to assign all of these individually to specific structures from the heterogeneous reaction products arising from peroxide cross-linking. Making full use of the scalar coupling between the two  $^{13}\text{C}$ -labeled positions C2 and C8, we are able to correlate some of the signals in the 2D INADEQUATE spectra. In such spectra  $J$ -coupled  $^{13}\text{C}$  nuclei share a common double-quantum (DQ) frequency along the vertical axis,<sup>15,12</sup> which helps to identify C2 and C8 signals belonging to the same chemical structure among the various structures formed during peroxide curing. This puts helpful constraints on the peak assignment because *pairs* of signals, rather than *individual* signals, have to be assigned. However, many of these signals have too low intensity, or the corresponding  $^{13}\text{C}$  spin coherence times, i.e., transversal relaxation times  $T_{2C}$ , in EPDM at 90 °C are too short to produce recognizable correlation signals in 2D NMR spectra. Such spectra thus yield an informative, but also selective,

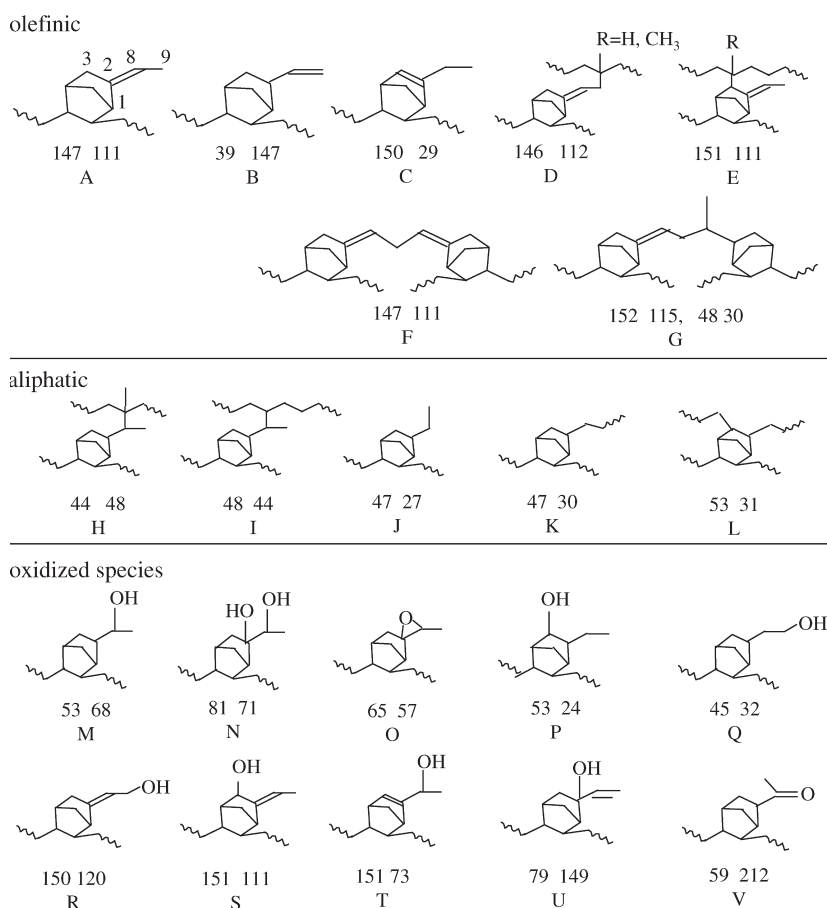


**Figure 4.** Predicted chemical shifts  $\delta_2$  and  $\delta_8$  of the  $^{13}\text{C}$  atoms at C2 and C8 position in ENB in various chemical structures considered in this paper. Predicted values were taken from the program CNMR db (ACD). Using the observed C2 and C8 signal positions for unmodified ENB in nonvulcanized EPDM as reference, a correction of +5 and -6 ppm was systematically applied to the predicted shift values of respectively tertiary and secondary olefinic  $^{13}\text{C}$  atoms. Predicted shift values of aliphatic  $^{13}\text{C}$  atoms were taken over without corrections. The predicted shifts do not take stereochemical effects (E/Z, endo/exo) into account. The shift prediction error is typically in the order of a few ppm.

picture of the chemical structures. The actual assignment of the signal pairs was carried out by comparing the chemical shifts with approximate values predicted from group-contribution calculations for a variety of hypothetical structures. A selection of these structures is illustrated together with the predicted shift values for the  $^{13}\text{C}$  atoms at C2 and C8 in Figure 4, but more were actually taken into account (Supporting Information, Table S1). We emphasize beforehand that the predicted shift values do not take stereochemical effects into account and are expected to be accurate within a few ppm only.

**Aliphatic Structures.** Figure 5 compares the aliphatic and olefinic ranges in Hahn-echo and INADEQUATE  $^{13}\text{C}$  NMR spectra of  $^{13}\text{C}$ -labeled EPDM before and after cross-linking as well as the corresponding spectra of the cross-linked rubber after the last step in the above-discussed stepwise peroxide cure. To discriminate between cross-linking and oxidation effects, the Hahn-echo spectrum of a peroxide-free EPDM sample which has been exposed to air at 175 °C is also shown.

At large magnification small signals are visible in addition to the major signals that were already discussed at the start of the Results section. In the aliphatic region (Figure 5, right), some of these arise from copolymer-chain sequences with propylene units separated by less than five monomers along the statistical copolymer chain, which causes secondary effects on the chemical shift of the carbon atoms in the ethylene and propylene monomers. A detailed analysis of

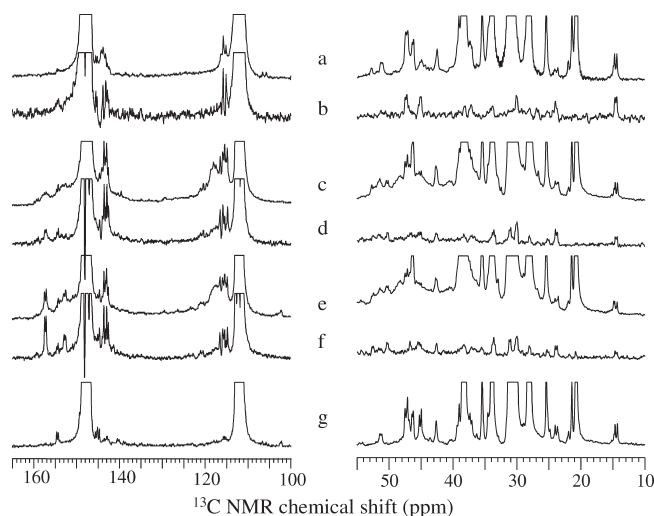


**Figure 5.** Modification of the ENB unsaturation and its conversion into aliphatic moieties upon peroxide cross-linking of EPDM. (left) Olefinic and (right) aliphatic part of (a, c, e, g) Hahn-echo and (b, d, f) INADEQUATE  $^{13}\text{C}$  NMR spectra of (a, b) non-cross-linked  $^{13}\text{C}$ -labeled EPDM, (c–f) cross-linked  $^{13}\text{C}$ -labeled EPDM peroxide-cured (c, d) in a single step of 17 min and (e, f) in four steps accumulating up to 19 min (to monitor double-bond conversion versus time), and (g) oxidized  $^{13}\text{C}$ -labeled EPDM exposed to air at 175 °C in the absence of peroxide. All spectra were recorded at 90 °C. For traces a–d the sample rotation rate was 4 kHz and for traces e–g 8 kHz.



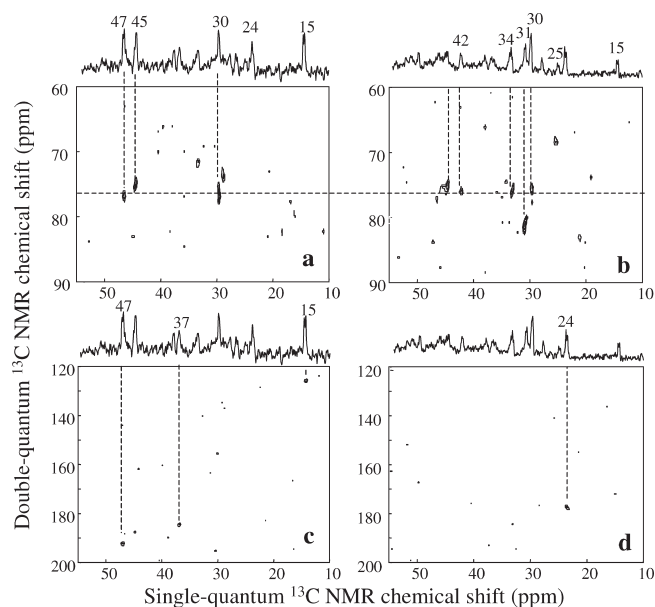


**Figure 6.** Aliphatic region in the 2D INADEQUATE  $^{13}\text{C}$  NMR spectra of  $^{13}\text{C}_2$ -ENB-EPDM. (a, b) Aliphatic–aliphatic and (c, d) aliphatic–olefinic correlations (a, c) before and (b, d) after peroxide cure. Neighboring  $^{13}\text{C}$  spin pairs at C2 and C8 in the various chemical structures formed share a common double-quantum signal. For comparison and reference purpose, the corresponding 1D INADEQUATE spectra are also indicated above the 2D spectra.

these signals is beyond the scope of this paper. Here we focus on  $^{13}\text{C}$  NMR signals, which are also visible in INADEQUATE spectra and thus must be related to the labeled C2 and C8 positions in ENB.

The natural-abundance signal of the ENB methyl carbon at C9 with its 100%  $^{13}\text{C}$  neighbor at C8 shows up at 15 ppm in all spectra. Its intensity in the Hahn-echo spectra of the three samples studied is always  $\sim 1\%$  of the combined peak area of the major olefinic E/Z doublets and thus decreases correspondingly upon cross-linking. On the basis of the previous assignment of ENB signals in the  $^{13}\text{C}$  NMR spectra of EPDM and a poly(ethylene-*co*-ENB) in solution,<sup>25</sup> similarly intense signals from the  $^{13}\text{C}$  atom at the C3 position in E and Z isomers should occur at  $\sim 37$  and  $40$  ppm, respectively, as well as of E- and Z-ENB C1 signals at 50 and 46 ppm. Indeed, the INADEQUATE spectrum of non-cross-linked EPDM contains signals at 37, 38, and 47 ppm, and in the Hahn-echo spectrum a partly resolved doublet at 51 ppm with a splitting of  $\sim 38$  Hz is visible. However, the latter signal does not survive the long filter time in the INADEQUATE pulse sequence. To check the assignment of the visible INADEQUATE signals, we have looked for correlations with the olefinic resonances at 111 and 147 ppm in the 2D INADEQUATE spectra (Figure 6). Despite the  $^{13}\text{C}$  labeling, it is extremely time-consuming to obtain sufficient signal-to-noise level to pick up the natural-abundance DQ signals of  $^{13}\text{C}$  nuclei at the allyl positions C1, C3, and C9. The fact that the DQ frequency of every spin pair should be equal to the sum of the frequencies of the two coupled  $^{13}\text{C}$  nuclei helps to identify the true signals in the 2D spectrum. The assignment of the signals at 47, 37, and 15 ppm to C1, C3, and C9 is confirmed by the observed corresponding DQ shift values 193, 185, and 126 ppm, reflecting the respective correlations to the Z-ENB signal C2 at 146 ppm, the E-ENB C2 signal at 147 ppm, and the C8 signal at 111 ppm (Figure 6c).

Additional signals are present in the INADEQUATE spectrum of non-cross-linked EPDM at 24, 30, 34, and 45

ppm. These are probably due to scrambling (few % peak height relative to the C2 and C8 signals at 147 and 111 ppm, respectively) of the  $^{13}\text{C}$  label during the ENB synthesis and its incorporation into EPDM as well as aging of the material since its synthesis in 1999. Peroxide cross-linking causes a range of new aliphatic signals as reflected by the broad inhomogeneous resonance between 10 and 70 ppm (Figure 2). Most of the better resolved allylic and impurity signals observed *before* cross-linking have become less intense *after* cross-linking. Exceptions are the 30 and 24 ppm signals, which have stayed constant, and the signal at 34 ppm, which has increased in intensity. From the new aliphatic signals after cross-linking we especially mention those at 25, 31, and 43 ppm. To assign at least some of these signals before and after cross-linking, we have also recorded 1D INADEQUATE spectra without proton decoupling, so that methylene and methine signals can be distinguished, and 2D INADEQUATE spectra, which reveal correlations between the signals of neighboring  $^{13}\text{C}$  nuclei. Without decoupling the signals at 45 and 47 ppm split up into doublets typical of  $J_{\text{CH}}$  coupling in  $^{13}\text{CH}$  moieties, while the 30 ppm signal becomes a triplet consistent with  $^{13}\text{CH}_2$ . The 2D INADEQUATE spectrum of the non-cross-linked EPDM shows separate correlations at DQ shifts  $\delta_m + \delta_n$  equal to 75 and 77 ppm between the  $\text{CH}_2$  resonance at 30 ppm, on the one hand, and each of the two CH signals at 45 and 47 ppm, on the other (Figure 6a). This points to chemical structures with saturated  $^{13}\text{CH}$ – $^{13}\text{CH}_2$  moieties, already present in EPDM before cross-linking. The 47 ppm signal was already assigned to Z-ENB C1 based on its correlation to the DQ shift of 192 ppm (see above). However, the additional DQ shift at 77 ppm indicates signal overlap at 47 ppm between the natural-abundance signal of C1 in Z-ENB and the  $^{13}\text{C}$ -labeled signal from another chemical species. After comparing the predicted  $^{13}\text{C}$  NMR shifts for C2 and C8 in various structures derived from the ENB units in EPDM (Figure 4), we tentatively assign these three signals to the endo and exo form of structure K, i.e., a saturated C2–C8 bond as part of an EPDM branch point. A possible explanation for such a saturated structure already present before cross-linking is that the  $^{13}\text{C}$ -labeled ENB, before it was built into the EPDM chain, still contained a small impurity (2–4%) of 5-vinyl-3-norbornene (VNB; structure B in Figure 4) from the last step in the synthesis.<sup>11</sup> During EPDM polymerization the endocyclic norbornene unsaturation of VNB is first incorporated into the main chain. The exocyclic unsaturated C8/C9 bond of VNB may then have taken part in the subsequent reaction, yielding a Y-type branch. Indeed, VNB is regularly added as a fourth monomer in ENB–EPDM polymerization to induce long-chain branching, which is beneficial for processing. However, it is commonly believed that the C8/C9 bond in the VNB monomers is incorporated into a second EPDM chain extending on both sides (H-type branch). To the best of our knowledge, however, no conclusive evidence exists that VNB produces H-type rather than Y-type branch points. H-type branches derived from VNB would expectedly have  $^{13}\text{C}$  NMR signals at ca. 49 and 40 ppm, and without proton decoupling these signals would split up into doublets. Such signals are not observed in the 1D and 2D INADEQUATE spectrum. Therefore, we tentatively suggest, that, when VNB is already part of a first EPDM chain via the endocyclic C5/C6 bond, the steric inaccessibility of the C8 position may cause the polymerization of the second EPDM chain to terminate at that position.

The same spectral region in the 2D INADEQUATE spectrum of cross-linked EPDM shows an additional pair

of signals at 34 and 43 ppm with roughly the same DQ shift  $\sim 77$  ppm as the above-discussed  $^{13}\text{CH}-^{13}\text{CH}_2$  moieties already present before cross-linking. Several possible substituent patterns at C3 and C9 of a saturated ENB species affect the shift values  $\delta_{\text{C}2}$  and  $\delta_{\text{C}8}$  in an opposite manner, resulting in a fairly constant DQ shift  $\delta_{\text{C}2} + \delta_{\text{C}8}$  (Figure 4; Table S1 in the Supporting Information). Comparing various options, we tentatively assign the new signals to an alcohol with the hydroxyl at C9 (structure Q in Figure 4), i.e., an oxidation product of the labile allylic C9 methyl of ENB. Likewise, the new signal at 25 ppm might be the C8 resonance of saturated ENB with a hydroxyl functionality at C3 (structure P). In the 2D INADEQUATE spectrum, however, this signal correlates with a DQ shift of 68 ppm, which is inconsistent with the predicted C2 shift  $\sim 53$  ppm for such a structure. Another new signal is found at 31 ppm. It correlates with a DQ shift of 82 ppm. This suggests a  $^{13}\text{CH}_2$  moiety coupled to a  $^{13}\text{C}$  atom with a shift of 51 ppm, but the corresponding signal does not appear above the spectral noise, probably as a result from its short  $^{13}\text{C}$  NMR coherence time  $T_2^*$ . According to chemical shift predictions, a  $^{13}\text{CH}-^{13}\text{CH}_2$  moiety with methine and methylene shifts of 51 and 31 ppm, respectively, is consistent with the doubly alkyl-substituted species (structure L in Figure 4). It is not obvious how such a structure may be formed along the commonly accepted pathways for peroxide curing, but we postpone this issue until the discussion of the reaction mechanism and possible side reactions in the next section.

**Olefinic Structures.** At the foot of the major olefinic doublets at 111 and 147 ppm in the EPDM spectrum *before* cross-linking, small overlapping signals occur in the regions 140–145 and 112–117 ppm (Figure 5). Some are due to the spinning sidebands of the major C8 and C2 signals, but the signal patterns cannot be explained by sidebands alone. The other signals, which comprise ca. 2% peak area of the E/Z-ENB signals at 147 ppm, reflect olefinic impurities, probably resulting from the synthesis, or aging since then. Because of the signal overlap and their low peak intensity, we do not attempt to assign the individual signals here. Peroxide cross-linking causes enhancement of signals in these two ranges and also yields new signals at the other (downfield) side of the major 147 ppm signal. These results indicate chemical pathways in peroxide curing which leave the double bond in ENB-EPDM intact but change the chemical structure near the double bond. To identify the structures formed, we have examined the olefinic regions in 2D INADEQUATE spectra, but the DQ frequencies of the new structures practically coincide with those of the major C2 and C8 signals, resulting in insufficient spectral resolution (Table S1 in the Supporting Information). However, clearly resolved cross-peaks are visible between the new olefinic signals in 2D TOCSY spectra (Figure 7). In this kind of 2D NMR experiment correlations between  $J$ -coupled  $^{13}\text{C}$  nuclei show up as off-diagonal cross-peaks between the autocorrelation signals at the respective single-quantum shift values along the spectral diagonal. The observed cross-peak between the new signals at 115 and 142 ppm is indicative of alkyl substitution at the C9 position with conservation of the unsaturated C2/C8 bond (structure D in Figure 4). Such a chemical structure is indicative for the combination of an EPM macroradical and an allylic C9 ENB-EPDM macroradical. Allylic combination represents a new pathway in the peroxide-curing mechanism and will be addressed in more detail at the end of the Discussion. According to chemical shift predictions, the new signals at the downfield side (higher shift values) of the 147 ppm resonance may well be due to olefinic C2 carbons with alkyl substitution at the C3 position (structure E in Figure 4).

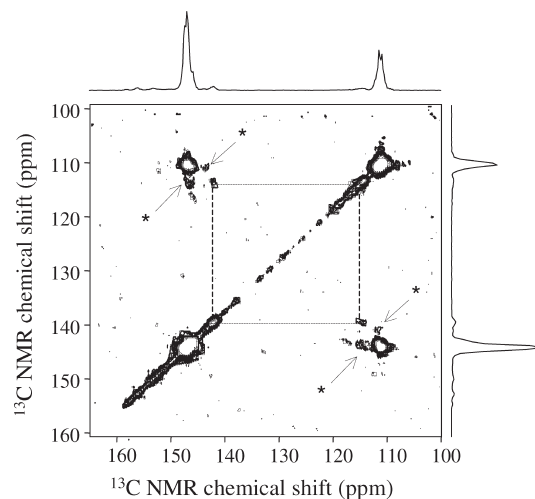


**Figure 7.** Olefinic-olefinic correlation region in the 2D TOCSY  $^{13}\text{C}$  NMR spectrum of single-step peroxide cross-linked  $^{13}\text{C}$ -labeled EPDM, showing correlations between signals of neighboring  $^{13}\text{C}$  nuclei coupled by the scalar coupling. Note the cross-peaks between the new signals at 142 and 115 ppm and the absence of (detectable) olefinic-olefinic cross-peaks associated with the new signals at 151 and 156 ppm. The spectrum has been symmetrized for enhancing the signal-to-noise ratio. Off-diagonal spinning sidebands associated with the 4 kHz sample rotation are marked with a star (\*).

This could be the combination product of an EPM and an allylic C3 ENB-EPDM macroradical. However, no cross-peaks to corresponding C8 signals are observed, which could confirm such interpretation. The lack of observable cross-peaks leaves room for an alternative assignment of the new C2 signals to other structures, such as an ENB isomer with the unsaturation between C2 and C3 (structure C), or an alcohol with the hydroxyl moiety at C3 (structure S). Such structures may respectively arise from resonance (double-bond delocalization) in C3 allylic ENB-EPDM macroradicals or from oxidation in the hot press.

**Oxidized Structures.** Peroxide-cured EPDM also shows new  $^{13}\text{C}$  NMR signals in the chemical shift ranges 55–85 and 170–220 ppm, which are respectively typical of  $^{13}\text{C}-\text{O}$  (alcohol, ether, epoxide) and  $^{13}\text{C}=\text{O}$  (carboxylic acid, keton, aldehyde) moieties (Figure 8). Note that several signals in these ranges of the  $^{13}\text{C}$  NMR spectra of EPDM before and after cross-linking are actually spinning sidebands of the major olefinic and aliphatic signals shown in Figure 5. The formation of alcohols as reaction products would also agree with the appearance of the new aliphatic signal at 34 and 43 ppm. Prior to the cross-linking, a number of signals are already present in these ranges, but these are spinning sidebands of aliphatic or olefinic carbon atoms. In addition to the known frequency separation from the centerbands, this is confirmed by their respective absence or dephasing in 1D INADEQUATE spectra, which were recorded without MAS synchronization. Most of the oxidation signals of the peroxide-cured EPDM are also found in the  $^{13}\text{C}$  NMR spectrum of  $^{13}\text{C}$ -labeled EPDM exposed to air at 175 °C in the absence of peroxide, which serves as a reference (Figure 8). Thus, the types of oxidized species formed under peroxide curing are comparable to those in EPDM aged in air. However, the degree of oxidation is strongly enhanced by the peroxide cure, as reflected by the particularly strong oxidation signals for the stepwise cross-linked EPDM used for the conversion study. Obviously, peroxide-induced EPDM macroradicals are much more sensitive to oxygen than the stable aliphatic and olefinic moieties along the EPDM chain. In fact, for the stepwise vulcanized EPDM



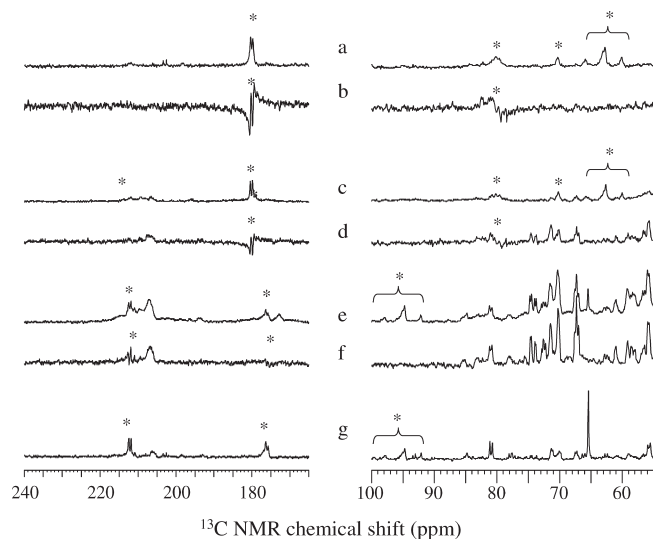


**Figure 8.** (left) Carbonyl and (right) alcohol/ether signals in (a, c, e, g) Hahn-echo and (b, d, f) INADEQUATE  $^{13}\text{C}$  NMR spectra of (a, b) non-cross-linked EPDM, EPDM peroxide-cross-linked in (c, d) a single step of 17 min and (e, f) in four steps accumulating up to 19 min to monitor double-bond conversion at intermediate times, and (g) oxidized EPDM exposed to air at 175  $^{\circ}\text{C}$ . All spectra were recorded at 90  $^{\circ}\text{C}$ . Traces a–d were recorded with a MAS rate of 4 kHz and traces e–g with a MAS rate of 8 kHz. Spinning sidebands are indicated with a star (\*).

some of the new  $^{13}\text{C}$ –O signals are even larger than the new aliphatic and olefinic signals discussed above. A significant part of the ENB double-bond conversion that we have above concluded from the decrease of the olefinic signals at 147 and 111 ppm may thus have resulted from oxidation. This is probably caused by the fact that the EPDM at intermediate cross-link states between subsequent cross-link steps was exposed to air and explains the high conversion seen with  $^{13}\text{C}$  NMR compared to the cross-link density estimated from  $^1\text{H}$  NMR  $T_2$  relaxometry. One would expect peroxide-enhanced oxidation of EPDM to start with the abstraction of labile hydrogen atoms at the tertiary and secondary carbon atoms in the EPM backbone or at the allylic C3 or C9 positions in the ENB monomers. Since both pathways involve natural-abundance  $^{13}\text{C}$  positions in our EPDM material; however, the small amounts of oxidized structures that are formed via these routes are not visible in the  $^{13}\text{C}$  NMR spectrum. Instead, almost all new oxidation signals originate from the  $^{13}\text{C}$ -labeled double bond directly, as further proven by the fact they practically all show up in the INADEQUATE spectra as well (Figure 9). The multiple new signals between 55 and 85 ppm are consistent with alcohol and epoxide structures such as M, N, and O in Figure 4 in various stereoisomeric forms as well as ethers and peroxides (not shown). Considering the high oxidation degree of the stepwise vulcanized EPDM as an artifact of the preparation procedure, for a more precise assignment of the oxidation signals we have focused on the peroxide-cured EPDM, which was vulcanized in a single step. Detailed analysis of the 2D INADEQUATE spectra (Figure 9) in combination with shift prediction for a range of possible oxidation species (Figure 4) reveals information about the signals at 56 and 67 ppm. The first is associated via the observed double-quantum shift 262 ppm to a ketone resonance at 206 ppm. This ketone signal falls outside the spectral width of the 2D spectrum, but it is indeed present in the 1D spectra and correlates in intensity with the signal at 55 ppm (Figure 8). This is indicative for a ketone species according to structure V in Figure 4. It is well-known that oxidation of unsaturated moieties in rubbers

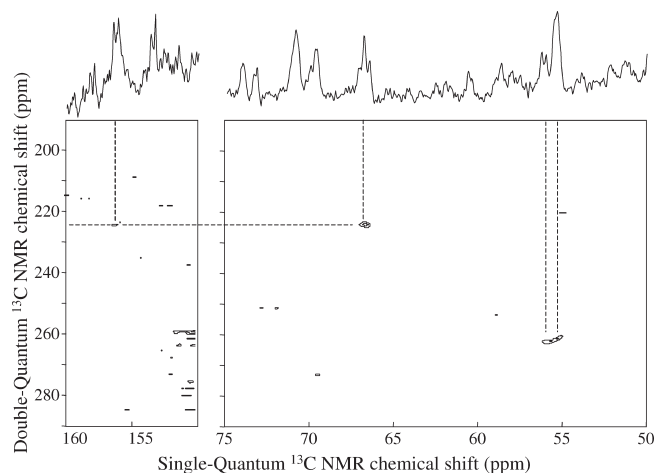


**Figure 9.** (left) Parts of the olefinic and (right) alcohol regions in the 2D INADEQUATE spectrum of single-step peroxide cross-linked  $^{13}\text{C}$ -labeled EPDM showing the correlation peaks associated with the new signals at 55, 67, and 157 ppm. The 1D INADEQUATE spectrum and the projection of the 2D spectra on the horizontal frequency axis are shown above the 2D spectra.

can produce ketones.<sup>36</sup> Further oxidation leads to breakage of the C2–C8 bond along with formation of carboxylic acid. Indeed, a carboxyl signal occurs at 170 ppm, which does not show up in 1D INADEQUATE spectra, as expected from such oxidation pathway in which the bond between C2 and C8 is broken.

Via the observed DQ shift of 224 ppm, the signal at 67 ppm appears to be coupled to an olefinic signal at 157 ppm. Indeed, a small signal just above the noise level is present at that position in the 2D INADEQUATE spectrum. The coupling of this olefinic carbon to a neighboring  $\text{sp}_3$  carbon is consistent with the absence of any cross-peak to this signal in the olefinic range of the TOCSY spectrum (Figure 7). Taking into account that the shift combination of 67 and 157 ppm must somehow be reconciled with the  $^{13}\text{C}$ -labeled positions C2 and C8, we tentatively assign these signals to a structure like T in Figure 4. Although unraveling the detailed oxidation pathways is beyond the scope of this paper, it is puzzling how such a structure could have formed from ENB in the presence of oxygen and peroxide. A possible explanation could be a contributing resonance structure of C3 allylic radicals with the double bond between C3 and C2 and the radical position at C8 (vide infra). In the presence of oxygen, the radical at this position has then become converted into an alcohol functionality at C8.

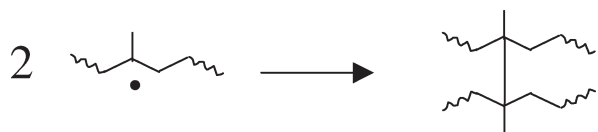
## Discussion

**Reaction Mechanism.** In the generally accepted mechanism of peroxide cross-linking of EPDM, the initial step is the decomposition of the peroxide into radicals, which abstract hydrogen atoms from the EPM backbone, resulting in the formation of EPDM macroradicals.

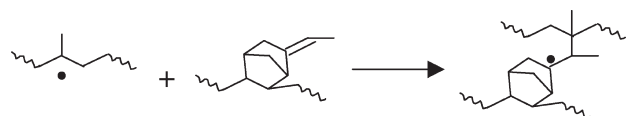


Radicals at the tertiary and secondary carbons in the EPM chain are more stable than those located at primary carbons. In principle, allyl radicals at the positions C3 and C9 in the ENB units are even more stable, but since the ENB monomers are only present at low concentration in the EPDM chains, for kinetic reasons, such allyl radicals are not expected to play an important role at this stage.<sup>6</sup>

In the next step the relatively stable macroradicals are supposed to react either by combination with each other

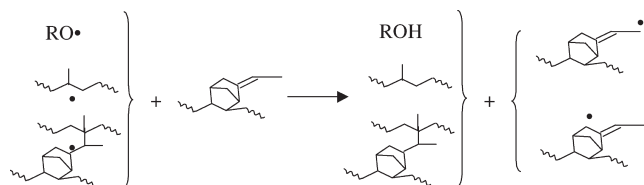


or by addition to the pendent unsaturation of the ENB units



In the addition case, steric hindrance probably prevents the newly formed macroradical to combine with another EPDM macroradical or to propagate further by adding to the double bond of a second ENB unit. Instead, addition cross-linking is terminated by hydrogen transfer from another (part of the) chain. In this way, aliphatic structures like H or I in Figure 4 are formed, and the radical is transferred to another position in the network, where it may form another cross-link. Addition thus results in a decrease of unsaturation and in the formation of new aliphatic structures. Indeed, the decrease of the olefinic C2 and C8 signals observed in our present study is consistent with such a picture, although the large conversion found for the stepwise cross-linked EPDM turned out to be substantially due to oxidation as well. More conclusive evidence could arise from the range of new aliphatic signals in 1D INADEQUATE spectra after peroxide cross-linking of the investigated EPDM with selectively  $^{13}\text{C}$ -labeled ENB, since these new signals can only come from aliphatic structures with saturated C2–C8 bonds. However, no resolved NMR signal pairs at 44 and 48 ppm, indicative for structures H and I, show up in the INADEQUATE spectra. This is remarkable because it seems inconsistent with the addition of EPDM macroradicals to the pendent ENB unsaturation as the major pathway, next to macroradical combination in the peroxide cure mechanism. It cannot be overemphasized, however, that the INADEQUATE NMR technique can only detect neighboring  $^{13}\text{C}$  nuclei with sufficiently long spin-coherence times  $T_{2\text{C}}$ . Especially, the  $^{13}\text{C}$  NMR signals of the cross-linked and thus more immobile parts of the rubber networks may well have too short  $T_{2\text{C}}$  relaxation times to show up in 1D and 2D INADEQUATE spectra.

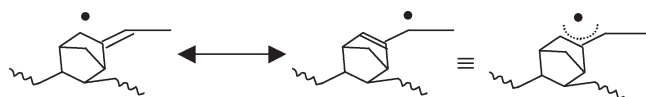
Interestingly, new olefinic signals show up in the  $^{13}\text{C}$  NMR spectra of cross-linked EPDM, which indicate that chemical-structure modifications also occur at the C3 and C9 positions next to the ENB unsaturation, but without the unsaturation being consumed. Most probably, hydrogen transfer reactions can take place from the ENB allylic positions C3 and C9 to radicals formed earlier in the peroxide curing of EPDM:



Allyl hydrogen atoms are more susceptible toward abstraction than aliphatic hydrogen atoms because of resonance stabilization of the allylic radicals. Combination of such

allylic ENB–EPDM macroradicals with aliphatic EPM radicals, or other allylic ENB–allyl radicals results in cross-links involving the ENB unsaturation without consuming it (e.g., structures D, E, and F in Figure 4). The TOCSY cross-peaks between new olefinic signals at 115 and 142 ppm provide evidence for allyl–alkyl combination at C9 (structure D). New C2 signals at 151 and 152 ppm may also indicate such combination at C3 (structure E). However, the expected correlation with a C8 signal at 111 ppm is not observed. Once formed, allylic radicals could also add to the unsaturation in other ENB units (structure G). Thus, the generally accepted mechanism, in which the ENB unsaturation only plays a role as a site for addition, has to be extended with a second pathway involving allylic radicals and their consecutive combination with other radicals. This is in accordance with the results of recent study with low-molecular-weight model compounds.<sup>7</sup> Our present  $^{13}\text{C}$  NMR study shows that allylic radicals also play an important role in the mechanism for peroxide cure of polymeric EPDM with realistic molecular weights. The fact that allylic modification shows up so prominently in our present study suggests that the allyl radicals are not mainly created by the short-lived primary peroxide radicals at the initial stages of the peroxide cure, but by the more stable EPDM macroradicals formed at later stages. Once formed, the allylic radicals are also sensitive to oxidation, which could explain the observed olefinic signals downfield of the major C2 signal assigned to a chemical structure with an alcohol moiety at C3 of C9 (structures R and S). However, no TOCSY cross-peaks were observed between C2 signals with shifts > 150 ppm and C8 signals at the expected positions 120 and 11 ppm, which could corroborate such interpretation.

The fact that the new C2 signals at 151 and 157 ppm show no TOCSY correlations to other olefin signals leaves room for speculation about reactions of different resonance structures of the allylic radical according to



Oxidation may then lead to an alcohol at C8 and a double bond between the C2 and the natural-abundance C position C3 (structure T). Evidence for such structure arises from correlation peaks in 2D INADEQUATE spectra between alcohol and olefin  $^{13}\text{C}$  NMR signals at 67 and 157 ppm, respectively. Resonance for the allylic ENB–EPDM macroradical may have also played a role in formation of the aliphatic structure L, showing up in the 2D INADEQUATE spectrum of cross-linked EPDM. It may have been formed in a multistep way from an earlier alkyl–allyl cross-link structure D, involving hydrogen abstraction from C3, followed by a “rearrangement” of the unsaturation to the C2/C3 carbon positions and, finally, macroradical addition to this bond at position C3.

## Conclusions

[2,8- $^{13}\text{C}_2$ ] ENB–EPDM was cured with peroxide, and the resulting chemical structures were investigated by use of MAS  $^{13}\text{C}$  NMR. The ENB termonomers with their pendent unsaturation are generally thought to enhance peroxide cross-linking by offering addition sites for the EPDM macroradicals formed shortly after the peroxide decomposition. Indeed, peroxide cure partly converts the pendent unsaturation of the ENB unit into a range of aliphatic structures with overlapping  $^{13}\text{C}$  NMR signals, visible in 1D INADEQUATE spectra. Using the 2D  $^{13}\text{C}$ – $^{13}\text{C}$

correlation NMR techniques INADEQUATE and TOCSY, we were able to identify some of the more mobile, new structures with long  $^{13}\text{C}$  spin-coherence times  $T_{2\text{C}}$ . An attempt was made to correlate the conversion of the ENB unsaturation at subsequent stages of the peroxide cure, as reflected by MAS  $^{13}\text{C}$  NMR spectroscopy, to the cross-link density estimated from  $^1\text{H}$  NMR  $T_2$  relaxometry. However, the stepwise-cured EPDM turned out to be oxidized relatively strongly, probably as a result of the presence of EPDM radicals at the intermediate curing stages and the repeated exposure to air between the cross-linking steps. Thus, significant part of the double-bond conversion observed with  $^{13}\text{C}$  NMR was caused by oxidation. In addition to the conversion of the unsaturated ENB units into new aliphatic cross-links and oxidized species, we have also observed new olefinic signals after peroxide cure, consistent with substitution at the allylic positions C9 and, possibly, C3 in ENB. Apparently, the ENB unsaturation is not only involved in the generally accepted cross-linking pathway via addition but also in a novel pathway in which cross-linking occurs via hydrogen abstraction at the allylic positions and consequent combination with other aliphatic or allylic EPDM macroradicals. This confirms that the allyl pathway observed in a recent low-molecular-weight model study<sup>7</sup> plays a significant role in the peroxide cure of real, high-molecular-weight EPDM as well (Figure S2, Supporting Information).

**Acknowledgment.** This work is part of the research program of the Dutch Polymer Institute (project #511). The authors thank Brahim Mezari (Eindhoven University of Technology) for his assistance regarding the MAS  $^{13}\text{C}$  NMR experiments.

**Supporting Information Available:** A table with predicted  $^{13}\text{C}$  NMR chemical shifts for the  $^{13}\text{C}$ -labeled C2 and C8 positions in various saturated structures derived from the ENB moieties in EPDM, (2) the 2D TOCSY spectrum of non-cross-linked EPDM, and (3) an updated scheme of the pathways for peroxide-induced cross-linking of EPDM. This material is available free of charge via the Internet at <http://pubs.acs.org>.

## References and Notes

- Hofmann, W. *Rubber Technology Handbook*; Hanser Publishers: Munich, 1989.
- Riedel, J. A.; Vander Laan, R. Ethylene Propylene Rubbers. In *The Vanderbilt Rubber Handbook*, 13th ed.; R. T. Vanderbilt Co.: New York, 1973; p 123.
- Duin van, M. *KGK, Kautsch. Gummi Kunstst.* **2002**, *55*, 150.
- Duynstee, E. F. J. *KGK, Kautsch. Gummi Kunstst.* **1987**, *40*, 205.
- Winters, R.; Heinen, W.; Verbruggen, M. A. L.; Lugtenburg, J.; Duin van, M.; De Groot, H. J. M. *Macromolecules* **2002**, *35*, 1958.
- van Duin, M.; Coussens, B. (Re)evaluation of the Importance of Hydrogen Abstraction during Radical Grafting of Polyolefins“, 11th Polymer Processing Society meeting, Stuttgart, **1995**.
- Peters, R.; van Duin, M.; Tonoli, D.; Kwakkenbos, G.; Mengerink, Y. J.; van Benthem, R. A. T. M.; de Koster, C. G.; Schoenmakers, P. J.; van der Wal, S. J. *Chromatogr., A* **2008**, *1201*, 151.
- Zachary, M.; Camara, S.; Whitwood, A. C.; Gilbert, B. C.; van Duin, M.; Meier, R.; Chechik, V. *Eur. Polym. J.* **2008**, *44*, 1099.
- Orza, R. A.; Magusin, P. C. M. M.; Litvinov, V. M.; Duin van, M.; Michels, M. A. J. *Macromol. Symp.* **2005**, *230*, 144.
- Orza, R. A.; Magusin, P. C. M. M.; Litvinov, V. M.; Duin van, M.; Michels, M. A. J. *Macromolecules* **2007**, *40*, 8999.
- Heinen, W.; Ballijns, L. N.; Wittenburg, W. J. A.; Winters, R.; Lugtenburg, J.; Duin van, M. *Polymer* **1999**, *40*, 4353.
- Henseley, D. R.; Goodrich, S. D.; Harwood, H. J.; Rinaldi, P. L. *Macromolecules* **2004**, *27*, 2351.
- Savant, D. M.; Reddy, V. D.; McCord, E. F.; Rinaldi, P. L. *Macromolecules* **2007**, *40*, 4199.
- AKZO Chemicals Division, Rubber Chemicals, cross-linking peroxides.
- Bourdonneau, M.; Ancian, B. *J. Magn. Reson.* **1998**, *132*, 316.
- Rucker, S. P.; Shaka, A. J. *Mol. Phys.* **1989**, *68*, 509.
- Litvinov, V. M.; Dias, A. A. *Macromolecules* **2001**, *34*, 4051.
- Fry, C. G.; Lind, A. C. *Macromolecules* **1988**, *21*, 1292.
- Litvinov, V. M. *Spectroscopy of Rubbers and Rubbery Materials*; RAPRA Technology, 2002; p 353.
- Gotlib, Yu. Ya.; Lifshits, V. A.; Shevelev, V. A.; Lishanskii, I. A.; Balanina, I. V. *Polym. Sci. USSR* **1976**, *18*, 2630.
- Dluzneski, P. R. *Rubber Chem. Technol.* **2001**, *74*, 451.
- Bax, A.; Freeman, R.; Kempell, S. P. *J. Am. Chem. Soc.* **1980**, *102*, 4849.
- Kobuke, Y.; Fueno, T.; Furukawa, J. *J. Am. Chem. Soc.* **1970**, *92*, 6548.
- Fisher, J.; Gradwell, M. J. *Magn. Reson. Chem.* **1991**, *29*, 1068.
- Van der Velden, G. *Macromolecules* **1983**, *16*, 85.
- Wang, M.; Bertmer, M.; Demco, D. E.; Blümich, B. *J. Phys. Chem. B* **2004**, *108*, 10911.
- Carmen, C. J.; Harrington, C. E.; Wilkes, C. E. *Macromolecules* **1977**, *10*, 530.
- Randall, J. C. *Macromolecules* **1978**, *11*, 33.
- Saalwächter, K. *J. Chem. Phys.* **2004**, *120*, 454.
- Brereton, M. G. *Macromolecules* **1990**, *23*, 1119.
- Litvinov, V. M. *Macromolecules* **2006**, *39*, 8727.
- Gronski, W.; Hasenhiindl, H.; Freund, B.; Wolff, S. *KGK, Kautsch. Gummi Kunstst.* **1991**, *44*, 119.
- Mori, M.; Koenig, J. L. *Rubber Chem. Technol.* **1995**, *68*, 551.
- Pollard, M.; Klimke, K.; Graf, R.; Spiess, H. W.; Wilhelm, M. *Macromolecules* **2004**, *37*, 813.
- Zorine, V.; Magusin, P. C. M. M.; Van Santen, R. A. *J. Phys. Chem. B* **2004**, *108*, 5600.
- Vogel, L.; Gross, D. *KGK, Kautsch. Gummi Kunstst.* **1992**, *45*, 609.